

KOVALENKO BOGDAN

National Aerospace University – KhAI

<https://orcid.org/0000-0002-9360-0691>e-mail: [b.kovalenko@khai.edu](mailto:b.kovalenko@khai.edu)

LUKIN VOLODYMYR

National Aerospace University – KhAI

<https://orcid.org/0000-0002-1443-9685>e-mail: [v.lukin@khai.edu](mailto:v.lukin@khai.edu)

## ANALYSIS OF DISTORTIONS DUE TO BPG-BASED LOSSY COMPRESSION OF NOISE-FREE AND NOISY IMAGES

Compression algorithms have become a popular way to deal with the problem of rapidly increasing data volume produced by images from different sources. These algorithms can be divided into two groups called lossless and lossy compression. In the case of providing a high compression ratio, lossy compression is needed. The paper utilizes Better Portable Graphics (BPG) as one of the promising lossy compression coders. For compression procedures, noise presence plays an important role in the sense that noise can affect compression performance and resulting image quality. This article deals with an analysis of the statistical characteristics of distortions introduced due to image lossy compression by the BPG coder.

The subject of this paper is the statistical characteristics of distortions introduced due to lossy compression of noise-free and noisy grayscale images. The goal is to analyze the characteristics of distortions introduced by the BPG coder and provide information about residual noise that can appear due to the compression of noisy images. The task is to calculate the statistical characteristics of distortions for several cases (noise-free vs. compressed; noise-free vs. noisy-compressed; noisy vs. noisy-compressed), create histograms, and analyze their behavior.

The main results are the following. The properties of the introduced distortions have to be studied for the reasonable setting of the coder parameters and control of compressed image quality. We show that the distortions might have distribution close to a Gaussian but it can be also heavy-tailed. This depends on several factors including the noise presence in an image to be compressed, image complexity, and the coder parameter  $Q$ . The noise presence leads to specific properties of introduced distortions and residual noise that can be useful for further post-filtering of compressed noisy images.

**Keywords:** BPG coder, lossy image compression, distortion analysis, greyscale images.

KOVALENKO BOGDAN, LUKIN VOLODYMYR

Національний аерокосмічний університет ім. М.С. Жуковського "ХАІ"

### АНАЛІЗ СПОТВОРЕНЬ, СПРИЧИНЕНИХ BPG-СТИСНЕННЯМ З ВТРАТАМИ БЕЗШУМНИХ І ЗАШУМЛЕНИХ ЗОБРАЖЕНЬ

Алгоритми стиснення стали популярним способом вирішення проблеми швидкого збільшення обсягу даних, отриманих із зображень з різних джерел. Ці алгоритми можна розділити на дві групи, які називаються стисненням без втрат і стисненням з втратами. У випадку забезпечення вищого коефіцієнту стиснення потрібно використовувати стиснення з втратами. У статті використано Better Portable Graphic (BPG) як один з перспективних методів стиснення з втратами. Для процедур стиснення наявність шуму відіграє важливу роль у тому сенсі, що шум може впливати на якість стиснення та якість отриманого зображення. Ця стаття присвячена аналізу статистичних характеристик спотворень, що вносяться внаслідок стиснення зображень з втратами за допомогою кодера Better Portable Graphics (BPG).

Предметом дослідження є статистичні характеристики спотворень, що вносяться внаслідок стиснення з втратами напівтонових зображень з шумом та без шуму. Мета – проаналізувати характеристики спотворень, що вносяться BPG-кодером, та надати інформацію про залишкові шуми, які можуть з'являтися при стисненні зашумлених зображень. Завдання полягає в обчисленні статистичних характеристик спотворень для кількох випадків (без шуму проти стисненого; без шуму проти стисненого зображення з шумом; зображення з шумом проти зображення з шумом та стисненого), побудові гістограм та аналізі їхньої поведінки.

Основні результати полягають у наступному. Вивчено властивості внесених спотворень для обґрунтованого налаштування параметрів кодера та контролю якості стисненого зображення. Показано, що спотворення можуть мати розподіл, близький до гаусівського, але розподіл може мати і важкий хвіст. Це залежить від декількох факторів, включаючи наявність шуму в зображенні, що стискається, складність зображення та значення параметру кодера  $Q$ . Наявність шуму призводить до специфічних властивостей внесених спотворень та залишкового шуму, знання яких може бути корисними для подальшої пост-фільтрації стиснутих зображень з шумом.

**Ключові слова:** BPG-кодер, стиснення зображень з втратами, аналіз спотворень, напівтонові зображення.

### Problem overview

Compression has become an inalienable part of image processing nowadays [1]. This is because of several reasons. First, images are the one of the main parts of visual information transferred via networks and stored [2]. Second, in many areas, a huge number of images is produced, for example, this relates to remote sensing, advertising, medicine, and so on [3, 4]. So, to reduce the size of such data, compression methods and algorithms are used [5]. There are various techniques that can be applied to solve this task. All of them can be divided into two groups: lossless and lossy ones [6]. The key differences between these two groups are the compression ratio (CR) and introduced distortions. Lossy compression can provide significantly higher CR, but it also brings some information loss. In image compression, information loss might appear as artifacts, smoothed details, and so on [7]. As a result, there should be some trade-off between image quality and compression ratio. Such a trade-off depends

on the application since, in some situations, better quality is preferred whilst, in other applications, a smaller output size (a larger CR) is more important [8, 9].

There are applications where the quality of original and compressed images is not high (e.g., due to the noise presence) and such images require additional quality improvement. A solution in this case can be decompressed image post-filtering [10]. This procedure is often able to improve the overall image quality and makes the final image more acceptable for some applications. To maximize the positive effect of filtering, it is desired to know the exact type and properties of the noise present in the target image before and after lossy compression. That is why, this study aims to provide detailed information about distortions that lossy compression brings to an image.

Recall that the noise can be of different types and intensity. It can be visible or invisible [11]. As a result, noise affects distortions introduced by lossy compression of images in a different manner [12]. In addition, distortions depend on image complexity and the coder used. Here we consider the better portable graphics (BPG) coder [13], which is characterized by certain advantages compared to other modern lossy compression techniques.

### Analysis of recent sources

The influence of statistics of distortions due to lossy compression on image visual quality and classification accuracy has been already studied by Aiazzi et al [14, 15] and Lukin et al [16, 17]. Italian researchers [14, 15] considered the task of near-lossy compression of hyperspectral data to prevent classification accuracy reduction due to distortions. Statistical analysis for AGU and ADCT coders (<https://ponomarenko.info/#dow>) for grayscale noise-free images was performed in [16]. Both coders belong to the discrete cosine transform (DCT) based family of coders. The authors studied the statistical and spatial-spectral characteristics of distortions introduced by lossy compression and showed that distortion distribution is close to normal for small values of compression control parameters (CCP), but it can significantly differ from normal for large values of CCP. The dependence of distortion characteristics on the image complexity and structure has been recently demonstrated in [17].

Taking into account that the BPG coder also belongs to the DCT-based family of coders, it is expected to have similar distortions characteristics. It is also worth studying the case of noisy images, which was not considered in the previous research (taking into account the prevalence of noise-affected images in some real-life situations).

**The purpose of the work is:** to analyze the distortions introduced by lossy compression performed by the BPG encoder for noise-free images as well as for images corrupted by additive white Gaussian noise. In the first order, we determine are statistical characteristics Gaussian or non-Gaussian.

### Presentation of the main material

It was mentioned in the introduction that there are dependencies between image properties and compression results. For this study, we have used two images that can be treated as having simple and complex structures. The term “image complexity” can be described in various quantitative and qualitative ways. Verbally it can be described in the following way: an image is considered more simple if a larger percentage of its pixels correspond to image homogeneous (or, at least, quasi-homogeneous) regions. Quantitatively, the complexity of noise-free images can be characterized by entropy. Examples of simple and complex structure images used in our study are presented in Fig.1. The image Frisco represents an example of a simple structure image whilst the image fr01 is a complex structure one (contains considerably more pixels that correspond to edges, small-sized details, and textures).



Fig. 1. The used test images Frisco (a) and fr01 (b)

The reasons for studying the (BPG) coder were the following. First, this is a quite novel coder that aims to replace the widely used JPEG [13]. The BPG coder can provide a higher compression ratio for similar quality compared to JPEG. Second, it has native support of 8 to 14 bits per channel, as well as support for the same color formats as JPEG (grayscale, YCbCr 4:2:0, 4:2:2, 4:4:4). The compression control parameter that is used in this coder is called the Q parameter, and its higher values lead to higher values of CR, resulting in a downgrade in image quality. The values of parameter Q vary from 1 to 51. Third, it is also a well-studied coder; in our previous works,

the coder showed good results in lossy image compression and proved its effectiveness both in working with grayscale and color images corrupted by various types of noise [18, 19].

The overall method of distortion analysis for the noise absence case can be performed as follows: an initial noise-free 8-bit grayscale image that can be denoted as  $I_{ij}$ ,  $i = 1, \dots, N_i$ ;  $j = 1, \dots, N_j$  ( $N_i$  and  $N_j$  represent the size of the image); then compress this image with different values of the  $Q$  parameter. Each compressed image can be presented as  $I_{ij}^C(Q)$ ,  $i = 1, \dots, N_i$ ;  $j = 1, \dots, N_j$ ,  $N_i$  and  $N_j$ . As a result, the distortions obtained during lossy compression for specific values of  $Q$  can be described by differences

$$\Delta_{ij}(Q) = I_{ij} - I_{ij}^{TC}(Q),, i = 1, \dots, N_i; j = 1, \dots, N_j \tag{1}$$

where  $I_{ij}^{TC}$  compressed noise-free image.

The next step is to analyze the obtained array of differences (1). Such an analysis can be performed in different ways. One of them is to carry out simple statistical analysis, e.g., to obtain histograms of differences and to check whether or not the distributions follow the normal law. Additionally, it is worth calculating statistical parameters to answer some additional questions: how heavy is the tail of the distribution if it turns out to be non-Gaussian, and is the distribution symmetric? For this purpose, we further use such parameters as variance, mean, kurtosis, and skewness [20]. The two latter parameters have to be close to zero if the distribution of a random variable (random process) is close to normal.

It was said that we deal with multiple values (a certain range) of  $Q$  values. This is explained by two facts. First, in practice, one might need to provide different characteristics of compressed images depending on requirements and their priority. Second, for the case of noisy image compression, we have to pay the main attention to the neighborhood of the optimal operation point (OOP) [19] since it is of major practical value in real-life situations. That is why, we use values of  $Q$  that start at 15 and end at 40 with a step of 5.

First, let us start our analysis with the simple image Frisco where noise is absent. The calculated statistical parameters obtained for this case are presented in Table 1.

Table 1

**Statistical characteristics of distortions for the Frisco image**

Q	Kurtosis	Skewness	Mean	Variance
15	0.2003	-0.0021	-0.0026	0.5289
20	0.4136	0.0147	-0.0019	1.1677
25	0.9217	0.0125	-0.0204	2.5667
30	2.0129	0.0539	-0.0341	5.2719
35	3.4047	0.0835	-0.0880	10.6142
40	4.9193	0.2543	0.0062	22.5580

From data in Table 1, the following conclusions can be drawn: for  $Q$  equal from 15 to 20, the values of kurtosis are close to zero, as are the values of skewness, which means that the obtained distortions can be treated as Gaussian. With  $Q$  increasing, values of kurtosis start to increase as well. For  $Q = 25$ , kurtosis is about unity, and each next step increases the values of kurtosis by one. As a result, the distribution looks less and less like Gaussian. It also needs to be noted that the values of mean and skewness are close to zero for all considered cases of  $Q$ . Thus, we have a symmetric heavy-tailed distribution of introduced errors. Also, note that the variance of differences (mean square error (MSE) of introduced distortions) quickly increases with  $Q$  growth and the distortions become visible for  $Q=40$  (this usually happens if MSE exceeds 20).

The next studied situation is the compression of a more complex image. Statistical parameters for the obtained differences are presented in Table 2.

Table 2

**Statistical characteristics of distortions for the fr01 image**

Q	Kurtosis	Skewness	Mean	Variance
15	-0.0226	0.0037	-0.0155	0.5855
20	0.1362	0.0277	-0.0139	1.8969
25	0.3321	0.0465	-0.0505	6.0132
30	0.8125	0.0902	-0.0359	16.4319
35	1.6626	0.1742	-0.0735	41.4552
40	2.9806	0.2448	-0.1909	93.4525

In this case, the situation is similar except for the following points. Kurtosis is close to zero for a wide range of  $Q$  values (from 15 to 25), and it becomes close to unity for  $Q = 30$ . From these results, the following conclusion can be drawn – the distribution of distortions retains its Gaussian properties even for larger values of  $Q$  in comparison with the case of compression of simple stricture images. One more difference between simple and

complex structure image compression is that the variance of the differences is higher for complex images, especially for  $Q > 25$ .

The obtained conclusions can also be confirmed by analysis of the obtained histograms. For the Frisco image (Fig. 2), for  $Q$  equal to 30 and more, the distribution becomes non-Gaussian (heavy-tailed).

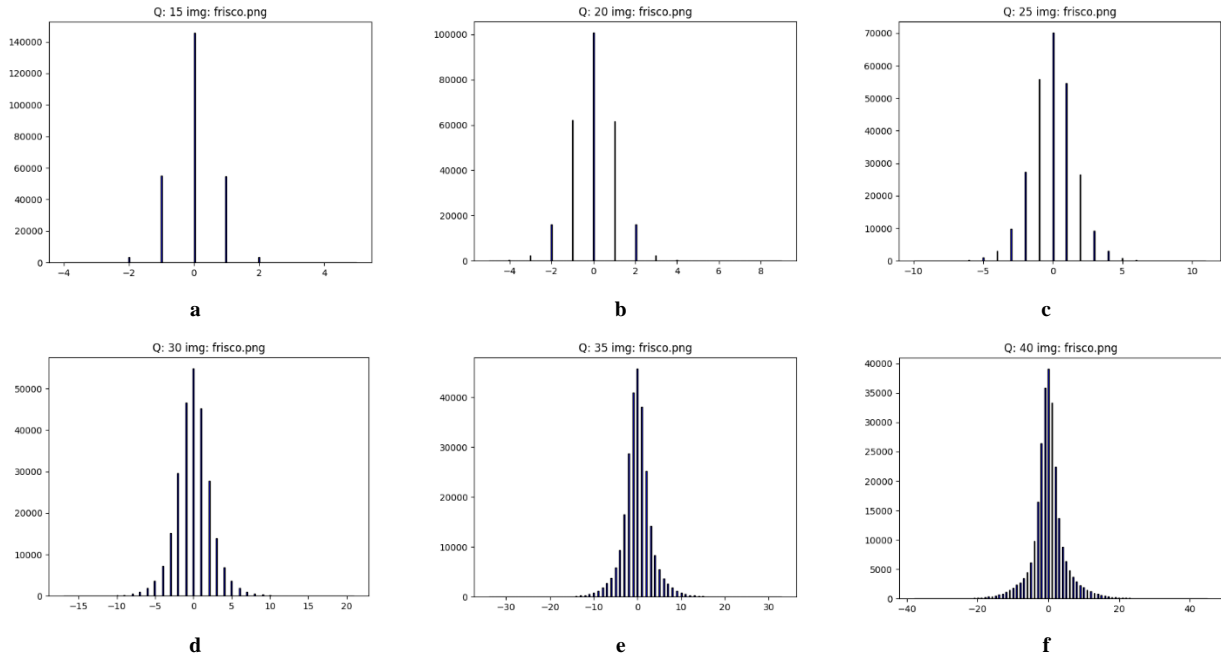


Fig. 2. The histogram of difference for the Frisco image for six values of  $Q$

The distributions of differences (1) obtained for compression of the fr01 image are presented in Fig.3.

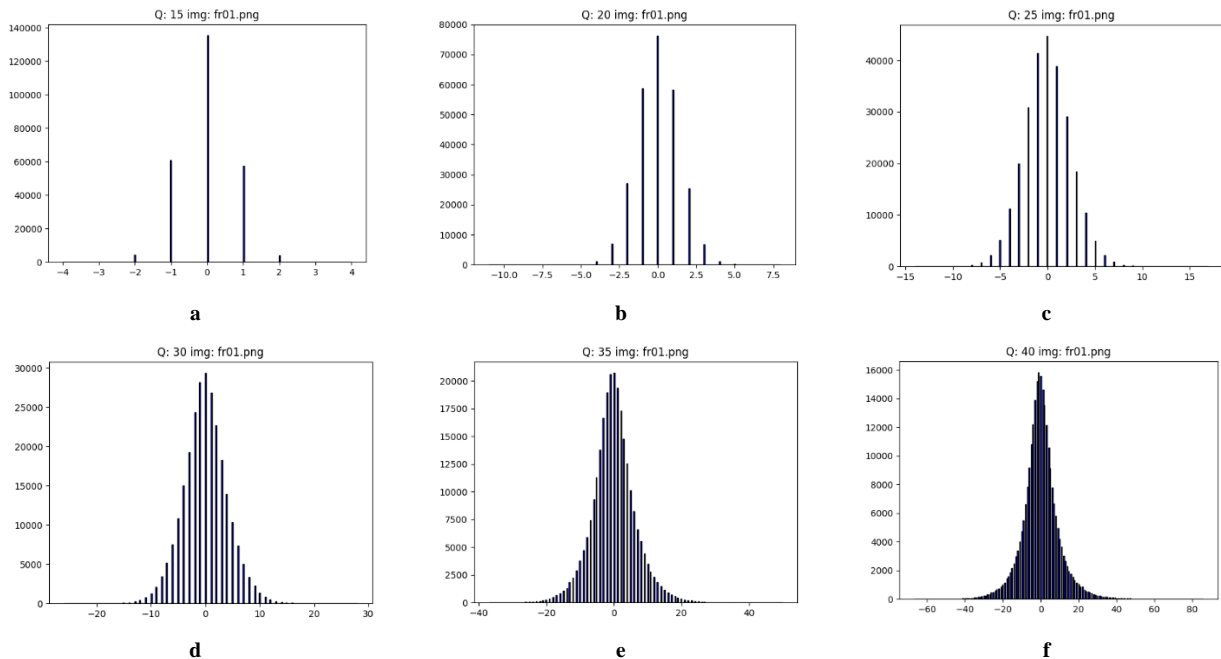


Fig. 3. The histograms of differences values for the fr01 image for six values of  $Q$

Overall, similar situations exist for the simple image. The distribution becomes less Gaussian with  $Q$  increasing. But in this case, the distributions are clearly non-Gaussian for larger  $Q$ .

The next step is to check if the noise that can be present (recall that, in real life, it is hard to acquire a noise-free image, except in the cases of computer-generated images) affects the behavior of distortions. In the case of noisy images, it is possible to use two ways of using the formula for differences (1). The first is to use (1) as it was previously (for noise-free images). In this case, an initial noise-free image compared to an image that was corrupted by noise and then compressed with some  $Q$  parameter. This allows studying the properties of residual noise in compressed images, this is important for the methods of compressed image post-filtering [10]. The second one is to

use  $I_{ij}^N$  (noised image) instead of  $I_{ij}$  (noise-free image); in other words, a compressed image is compared to the corresponding noisy image.

The first variant is to check what are the properties of combined distortions that is the joint influence of the noise and lossy compression. In the second case, the difference analysis characterizes the properties of distortions introduced by the encoder applied to noisy images or how the presence of noise in the image affects the distortions' distribution.

For noise simulation in this work, we have used additive white Gaussian noise (AWGN), which is known as one of the simplest noise models and a good starting point in research. Overall, according to the noise model, a noisy image can be described in the following way:

$$I_{ij}^n = I_{ij}^{true} + n_{ij}, \tag{2}$$

where  $I_{ij}^n$  denotes the noisy  $ij$ -th pixel value,  $I_{ij}^{true}$  is the true  $ij$ -th pixel value,  $n_{ij}$  is the value of AWGN having zero mean and the variance  $\sigma^2$ . Below we assume that noise variance is a priori known or accurately pre-estimated in advance.

Let us start from the first case when we add noise to the image and use the (1) formula, taking into account that now we compress the noisy image. As a result, the formula (1) can be changed in the following way:

$$\Delta_{ij}(Q) = I_{ij} - I_{ij}^{NC}(Q), \quad i = 1, \dots, N_i; \quad j = 1, \dots, N_j, \tag{3}$$

where  $I_{ij}^{NC}$  is the compressed noisy image.

First, let us look at the histograms obtained for this variant that are presented in Figs. 4–5. It is also important to note that the variance of AWGN is equal to 100 (in this case, the noise is visible in most noisy images).

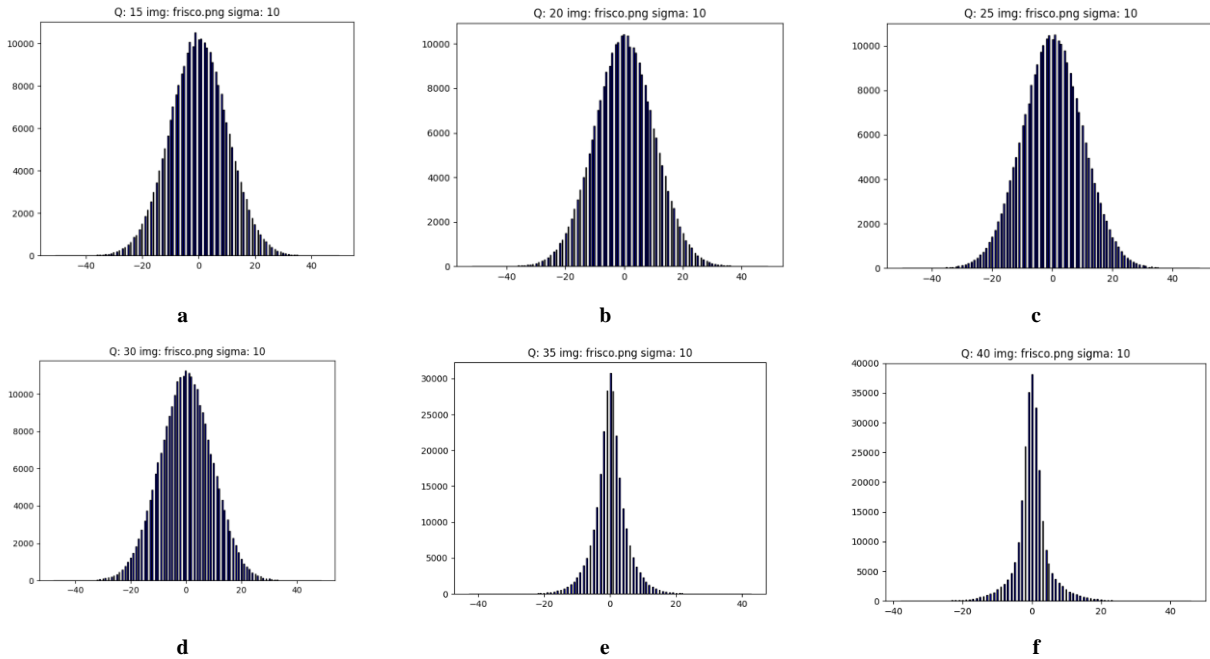


Fig. 4. The histograms of differences between the noise-free and compressed noisy images for the Frisco image

From the analysis of data in Fig. 4, it is possible to see that for  $Q$  in the range of 15 to 30, the distribution has a Gaussian shape. For larger  $Q$ , it seems that the residual noise in the compressed image starts to be non-Gaussian. The noise filtering effect due to lossy compression is observed for  $Q=35$  and  $Q=40$  where  $Q=35$  corresponds to the optimal operation point [10].

Table 3

Statistical characteristics of distortions (residual noise) for the noisy Frisco image

Q	Kurtosis	Skewness	Mean	Variance
15	0.0198	-0.0105	-0.0252	104.0136
20	0.0247	-0.0078	-0.0139	103.3174
25	0.0329	-0.0052	0.0046	100.1885
30	0.0419	-0.0079	0.0031	90.8979
35	2.6541	0.0054	-0.0148	24.9837
40	4.7843	0.2334	-0.0180	25.0086

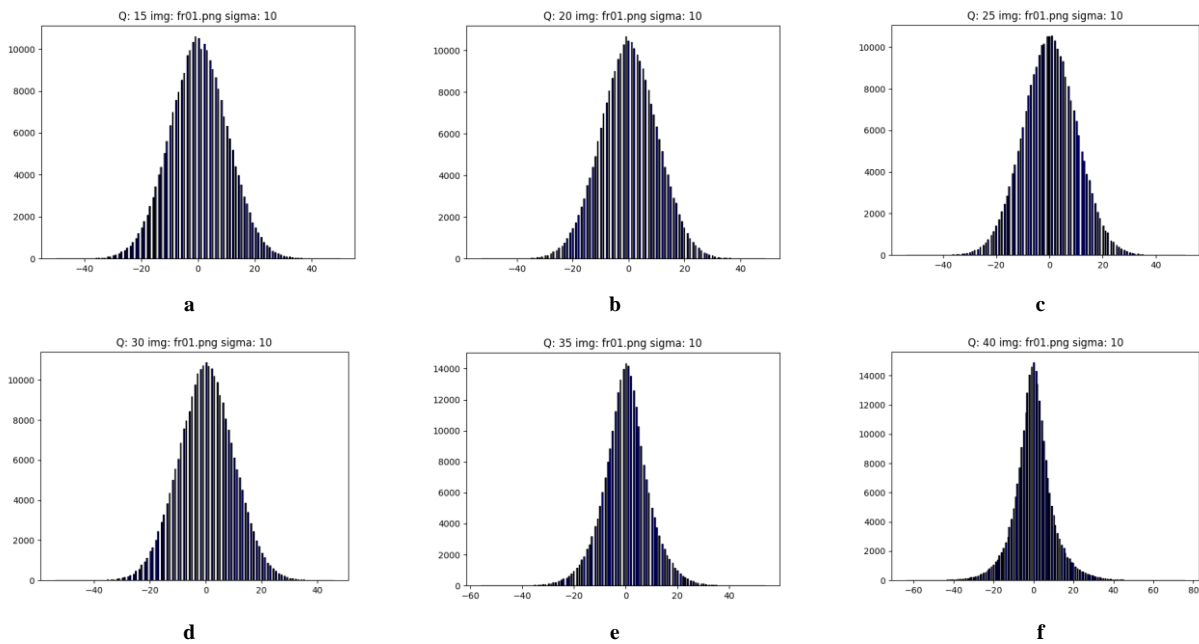


Fig. 5. The histograms of differences between the noise-free and compressed noisy images for the fr01 image

In the case of a more complex image (see data in Fig. 5), the tendencies are similar. This time the histograms might have additional or local peaks (are not as smooth as previously). The distributions in Figures 5,e, and 5,f seem narrower than for other histograms. This deals with partial noise suppression when lossy compression is applied to noisy images [10].

Table 4

Statistical characteristics of distortions (residual noise) for the noisy fr01 image

Q	Kurtosis	Skewness	Mean	Variance
15	0.0382	-0.0074	0.0285	103.3563
20	0.0389	-0.0079	0.0303	103.0498
25	0.0558	-0.0095	0.0535	101.6223
30	0.0716	-0.0077	0.0331	98.9175
35	0.9200	-0.0102	0.0107	77.7847
40	2.6319	0.1937	-0.0498	98.4561

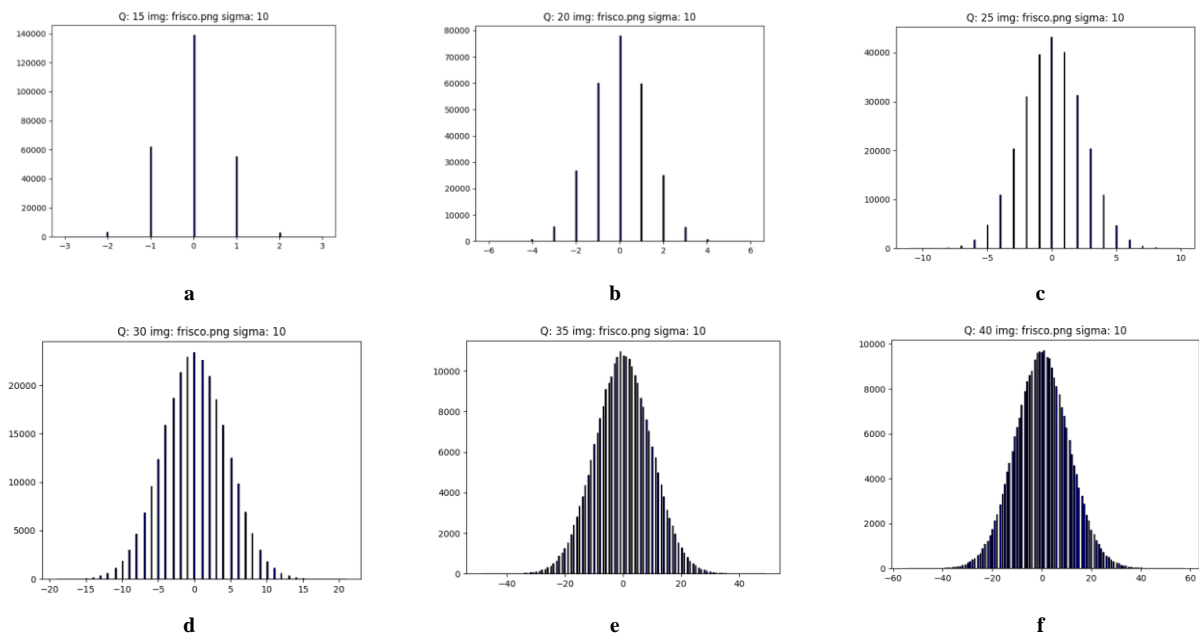


Fig. 6. The histogram of differences (3) for the noisy Frisco image

As one can see, the distributions seem to be close to Gaussian for almost all values of Q.

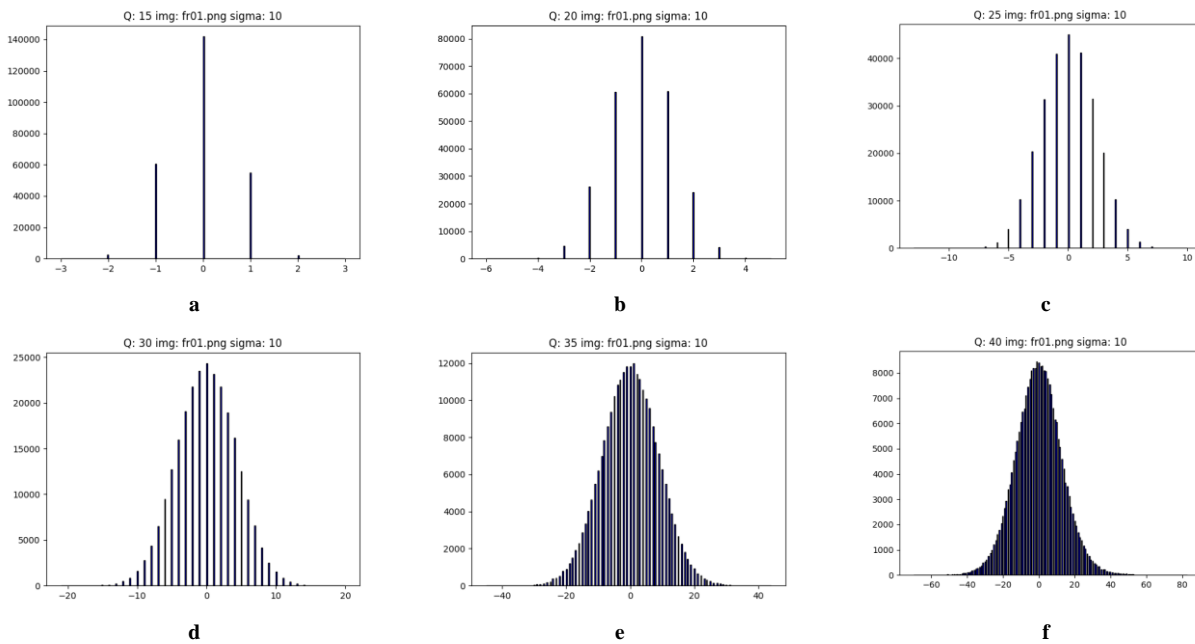


Fig. 7. The histogram of differences (3) for the noisy fr01 image

Preliminary conclusions that follow from histogram (Fig. 4 and 5) analysis are confirmed by statistical data presented in Tables 3 and 4. Kurtosis is close to zero for Q=30 and less. But it is not close to zero for Q=35 and 40 indicating non-Gaussian properties of residual noise. Another interesting moment is that the variance of distortions is smaller than the AWGN variance for Q=30, 35, and 40 – this is associated with the aforementioned noise filtering effect.

The final situation to be considered is when the differences obtained due to lossy compression for specific values of Q can be described as:

$$\Delta_{ij} = I_{ij}^N - I_{ij}^{NC}, \quad i = 1, \dots, N_i; \quad j = 1, \dots, N_j, \quad (4)$$

where  $I_{ij}^N$  is the noisy image (artificially noised image in our simulations) and  $I_{ij}^{NC}$  is the compressed noisy image. The histograms of  $\Delta_{ij}$  are presented in Fig. 6, and Fig 7. Overall, at the first glance, for both images, it appears that distortions are more Gaussian-like than those shown previously.

The statistical parameters (presented in Tables 5 and 6) prove that statement. For the simple structure image, the kurtosis and skewness is close to zero for all values of Q. The complex structure image (see data in Table 6) shows similar results except for Q equal to 40.

Table 5

Statistical characteristics of distortions for the noisy Frisco image

Q	Kurtosis	Skewness	Mean	Variance
15	-0.1551	0.0260	-0.0276	0.5396
20	-0.1021	0.0022	-0.0162	1.7164
25	-0.0656	-0.0058	0.0023	5.6524
30	-0.0310	-0.0002	0.0008	19.8241
35	0.0331	0.0017	-0.0171	94.6806
40	0.1052	0.0188	-0.0204	120.9301

Table 6

Statistical characteristics of distortions for the noisy fr01 image

Q	Kurtosis	Skewness	Mean	Variance
15	-0.2062	0.0179	-0.0243	0.5137
20	-0.1956	-0.0134	-0.0225	1.5821
25	-0.1404	-0.0012	0.0007	5.1657
30	-0.0633	-0.0076	-0.0197	18.3098
35	0.0621	-0.0036	-0.0421	78.5642
40	0.5193	0.0802	-0.1026	169.9732

### Conclusions

In this study, we have analyzed the characteristics of distortions due to lossy image compression by the Better Portable Graphics coder. The cases of noisy and noise-free images are also considered. It is shown that for the noise-free images, as Q increases, the introduced distortions tend to become non-Gaussian. This starts to happen for

Q about 30. For larger Q, the distribution of distortions becomes non-Gaussian.

It is also shown that the presence of noise in an image to be compressed affects the distortion introduced by the considered encoder. In this paper, the noise model used was AWGN, and as a result, the combined distortions are mostly close to Gaussian, especially when comparing a noisy image with a compressed one.

Further research steps can deal with the development of an approach to post-filtering that takes into account the information about distortions obtained due to compression to increase the overall quality of the final (compressed) image.

## References

1. Shelke S. K., Sinha S. K., Patel G. S. Study of End to End Image Processing System Including Image De-noising, Image Compression & Image Security. *Wireless Pers Commun.* 2021. Volume 121. P. 209–220. DOI: <https://doi.org/10.1007/s11277-021-08631-9>.
2. Pan S., Jiang J., Qiu H., Qiao J., Xu M. Research on Mass Image Data Storage Method for Data Center. *3D Imaging—Multidimensional Signal Processing and Deep Learning. Smart Innovation, Systems and Technologies*, 2023. Volume 349. DOI: [https://doi.org/10.1007/978-981-99-1230-8\\_6](https://doi.org/10.1007/978-981-99-1230-8_6).
3. Monika R., Dhanalakshmi S. An efficient medical image compression technique for telemedicine systems. *Biomedical Signal Processing and Control*, 2023. Volume 80, part 2. DOI: <https://doi.org/10.1016/j.bspc.2022.104404>.
4. Alam F., Ofli F. & Imran M. Processing Social Media Images by Combining Human and Machine Computing during Crises. *International Journal of Human–Computer Interaction*, 2018. Volume 34. Issue 4. P. 311–327. DOI: 10.1080/10447318.2018.1427831
5. Fu C., Du B. Remote Sensing Image Compression Based on the Multiple Prior Information. *Remote Sensing*, 2023. Volume 15. No. 8. DOI: <https://doi.org/10.3390/rs15082211>.
6. Hussain A. J., Al-Fayadh A., Radi N. Image compression techniques: A survey in lossless and lossy algorithms. *Neurocomputing*, 2018. Volume 300. P. 44–69.
7. Sultana Z., Nahar L., Tasnim F., Hossain M. S., Andersson K. Lossy Compression Effect on Color and Texture Based Image Retrieval Performance. *Intelligent Computing & Optimization. ICO 2022. Lecture Notes in Networks and Systems*, 2023. Volume 569. DOI: [https://doi.org/10.1007/978-3-031-19958-5\\_108](https://doi.org/10.1007/978-3-031-19958-5_108).
8. Veena S., Rao M. Handling Tradeoff Between Visual Perception and Compression in Video Codec Using Optimal Intra-Frame Prediction. *Wireless Pers Commun.* 2021. Volume 119. P. 1515–1540. DOI: 10.1007/s11277-021-08293-7.
9. Setiawan I., Dahlan R., Basuki A. I., Susanto H., Rosiyadi D. Trade-off between Image Quality and Computational Complexity: Image Resizing Perspective. *Jurnal Teknik Elektro*, 2022. Volume 14. No. 1. P. 24–28. DOI: <https://doi.org/10.15294/jte.v14i1.37629>.
10. Kovalenko B., Rebrov V., Lukin V. Analysis of the potential efficiency of post-filtering noisy images after lossy compression. *Ukrainian journal of remote sensing*, 2023. Volume 10. No. 1. DOI: 10.36023/ujrs.2023.10.1.231.
11. Chatterjee P., Milanfar P. Is Denoising Dead? *IEEE Transactions on Image Processing*, 2010. Volume 19. No. 4. P. 895–911. DOI: 10.1109/TIP.2009.2037087.
12. Al-Chaykh O. K., Mersereau R. M. Lossy compression of noisy images. *IEEE Transactions on Image Processing*, 1998. Volume 7. No. 12. P. 1641–1652.
13. Albalawi U., Mohanty S., Kougianos E. A Hardware Architecture for Better Portable Graphics (BPG) Compression Encoder. *2015 IEEE International Symposium on Nanoelectronic and Information Systems*, 2015. P. 291–296. DOI: 10.1109/iNIS.2015.12.
14. Aiazzi B., Baronti S., Santurri L., Selva M., Alparone L. Impact of irreversible data compression on spectral distortion of hyper-spectral data. *Geoinformation for European-wide Integration*, 2003. ISBN 90-77017-71-2.
15. Aiazzi B., Alparone L., Baronti S., Lastri C., Selva M. Spectral Distortion in Lossy Compression of Hyperspectral Data. *Journal of Electrical and Computer Engineering*, 2012. Volume 2012. Article ID 850637. DOI: <https://doi.org/10.1155/2012/850637>.
16. Shvec I., Lukin V. Analiz karakteristik iskazhenij pri szhatii izobrazhenij sovremennymi metodami na osnove dcp [Analysis of distortion characteristics in image compression by modern dcp-based methods]. *Aviacionno-kosmicheskaya tehnika i tehnologiya*, 2017. No. 2. Issue 137. ISSN – 1727-7337.
17. Abramova V., Lukin V., Abramov S., Abramov K., Bataeva E. Analysis of Statistical and Spatial Spectral Characteristics of Distortions in Lossy Image Compression. *2022 IEEE 2nd Ukrainian Microwave Week (UkrMW)*, 2022. P. 644–649. DOI: 10.1109/UkrMW58013.2022.10036949.
18. Kovalenko B., Lukin V., Vozel B. BPG-Based Lossy Compression of Three-Channel Noisy Images with Prediction of Optimal Operation Existence and Its Parameters. *Remote Sensing*, 2023. Volume 15. No. 6. DOI: <https://doi.org/10.3390/rs15061669>.
19. Lukin V., Kovalenko B., Vozel B. A Fast and Accurate Prediction of BPG Compression Parameters in Optimal Operation Point Neighbourhood for Three-channel Noisy Images. *Fundamental Research and Application of Physical Science*, 2023. Volume 8. P. 129–160. DOI: <https://doi.org/10.9734/bpi/fraps/v8/7110A>.
20. Ranganathan P., Gogtay N. An Introduction to Statistics - Data Types, Distributions and Summarizing Data. *Indian Journal of Critical Care Medicine*, 2019. Volume 23. P. 169–170. DOI: 10.5005/jp-journals-10071-23198.